Maximum A Posteriori Probability Estimation of Integer Ambiguities and Baseline

Patrick Henkel (*,**) and Jane Jean Kiam (**)
* Technische Universität München, Munich, Germany
** Advanced Navigation Solutions - ANAVS, Munich, Germany
patrick.henkel@tum.de, jane.kiam@anavs.de

Abstract – In this paper, a maximum a posteriori probability estimator is derived for determining the relative position and carrier phase integer ambiguities with GPS carrier phase measurements. The estimator is also applied to real measurements and enabled a heading determination with an accuracy of $0.5^\circ/$ baseline length [m].

Keywords – Carrier phase positioning, Integer Ambiguity Resolution, MAP Estimation, Heading determination.

I. Introduction

The carrier phase of GPS/ Galileo satellite signals can be tracked with millimeter accuracy but is periodic which results in an integer ambiguity for each satellite. In this paper, we focus on attitude determination and, therefore, consider only double difference (DD) measurements between two receivers. The DD eliminates the receiver/ satellite clock offsets, biases and also the atmospheric delays. The DD phase measurements for the satellite pair $\{k,l\}$ are modeled at time t as in [1] as

$$\begin{aligned}\lambda/2\pi \cdot \left((\varphi_1^{kl}(t+\delta\tau_1)) - (\varphi_2^{kl}(t+\delta\tau_2))\right)\\ \approx (\vec{e}^{\,kl}(t+\delta\tau_2))^{\mathrm{T}}\vec{b}_{12}(t+\delta\tau_2)\\ + c_{12}^{kl}(t,\delta\tau_1,\delta\tau_2) + \lambda N_{12}^{kl} + \varepsilon_{12}^{kl}(t+\delta\tau_1, t+\delta\tau_2),\end{aligned} \quad (1)$$

with the wavelength λ, the receiver clock offset $\delta\tau_r$, the unit vector $\vec{e}^{\,k}$ pointing from the k-th satellite to the receivers, the baseline vector $\vec{b}_{12}$ between both receivers, the DD correction c_{12}^{kl}, the integer ambiguity N_r^k and the phase noise ε_r^k. The double indices $\{kl\}$ and $\{12\}$ indicate differencing between two satellites/ receivers.

The correction in Eq. (1) is required for low-cost GPS receivers where the oscillators show clock offsets in the order of milliseconds: The satellite movement within the time of the differential receiver clock offset is no longer negligible. The correction was derived by Henkel et al. in [1] to maintain the integer property of ambiguities. It is given by

$$\begin{aligned}&c_{12}^{kl}(t,\delta\tau_1,\delta\tau_2)\\ &= (\vec{e}_1^{\,k}(t+\delta\tau_1))^{\mathrm{T}}\left(\vec{x}_1(t+\delta\tau_1) - \vec{x}^{\,k}(t+\delta\tau_1-\Delta\tau_1^k)\right)\\ &- (\vec{e}_1^{\,l}(t+\delta\tau_1))^{\mathrm{T}}\left(\vec{x}_1(t+\delta\tau_1) - \vec{x}^{\,l}(t+\delta\tau_1-\Delta\tau_1^l)\right)\\ &- (\vec{e}_1^{\,k}(t+\delta\tau_2))^{\mathrm{T}}\left(\vec{x}_1(t+\delta\tau_2) - \vec{x}^{\,k}(t+\delta\tau_2-\Delta\tau_2^k)\right)\\ &+ (\vec{e}_1^{\,l}(t+\delta\tau_2))^{\mathrm{T}}\left(\vec{x}_1(t+\delta\tau_2) - \vec{x}^{\,l}(t+\delta\tau_2-\Delta\tau_2^l)\right),\end{aligned} \quad (2)$$

with $\Delta\tau_r^k$ being the signal propagation time from the satellite to the receiver. The corrected DD phase measurements can then be modeled in matrix-vector notation as

$$\tilde{\Psi} = H\xi + AN + \eta, \quad (3)$$

where all variables are implicity defined by Eq. (1). The measurement model of Eq. (3) is quite general and also allows a stacking of code measurements in $\tilde{\Psi}$. It is also common practice to include measurements from multiple epochs.

Teunissen has developed in [2] the LAMBDA method to solve the integer least-squares problem for GPS. In [3], he proposed a constrained LAMBDA method which takes a priori information on the baseline length into account. Multi-frequency linear combinations are also an attractive means to eliminate the ionospheric delay and to increase the wavelength and, thereby, to improve the reliability of integer ambiguity resolution as described by the author in [4]- [6].

II. MAP Estimation of Baseline and Integer Ambiguities

A. Initial ambiguity fixing by Tree search

The Maximum Likelihood (ML) estimator determines the baseline and ambiguity parameters $\{\xi, N\}$ that have generated the measurements $\tilde{\Psi}$ with largest probability, i.e.

$$\max_{\xi,N} P(\tilde{\Psi}|\xi,N). \quad (4)$$

The Maximum A Posteriori Probability (MAP) estimator is the complement to the ML estimator and maximizes the probability $P(\xi,N|\tilde{\Psi})$ of the baseline and ambiguity parameters for a given set of measurements. The MAP estimator can be related to the ML estimator with the rule of Bayes $P(\tilde{\Psi}|\xi,N)P(\xi,N) = P(\xi,N|\tilde{\Psi})P(\tilde{\Psi})$, i.e. it is given by

$$\max_{\xi,N} P(\xi,N|\tilde{\Psi}) = \max_{\xi,N} \frac{P(\tilde{\Psi}|\xi,N)P(\xi,N)}{P(\tilde{\Psi})}, \quad (5)$$

where $P(\xi,N)$ denotes the a priori information on ξ and N, and $P(\tilde{\Psi})$ is considered as a marginal distribution. Assuming that the distribution of the measurement noise $P(\tilde{\Psi}|\xi,N)$ is Gaussian and that the a priori information is statistically independent and also Gaussian distributed as $P(\xi,N) \sim \mathcal{N}(\bar{\xi}, \Sigma_{\bar{\xi}})$, the maximization can also be written as a minimization, i.e.

$$\min_{\xi,N}\left(\|\tilde{\Psi} - H\xi - AN\|^2_{\Sigma_\Psi^{-1}} + \|\xi - \bar{\xi}\|^2_{\Sigma_{\bar{\xi}}^{-1}}\right). \quad (6)$$

The minimization over the integer-valued N requires a search. Assuming a search space volume χ^2, the search determines all integer candidate vectors inside χ^2, i.e.

$$\min_{\xi}\left(\|\tilde{\Psi} - H\xi - AN\|^2_{\Sigma_\Psi^{-1}} + \|\xi - \bar{\xi}\|^2_{\Sigma_{\bar{\xi}}^{-1}}\right) \le \chi^2. \quad (7)$$

Teunissen decomposed the first term of Eq. (7) into three orthogonal terms in [2], i.e.

$$\begin{aligned}\|\tilde{\Psi} - H\xi - AN\|^2_{\Sigma_\Psi^{-1}} &= \|\hat{N} - N\|^2_{\Sigma_{\hat{N}}^{-1}} + \|\check{\xi}(N) - \xi\|^2_{\Sigma^{-1}_{\check{\xi}(N)}} \\ &\quad + \|P_{\bar{A}}^{\perp} P_H^{\perp} \tilde{\Psi}\|^2_{\Sigma_\Psi^{-1}}, \end{aligned} \tag{8}$$

where $P_H^{\perp}$ is the orthogonal projector on the space of H and $\bar{A} = P_H^{\perp} A$. The last term of Eq. (8) denotes the irreducible noise. The unconstrained least-squares float ambiguity estimate $\hat{N}$ and the unconstrained least-squares fixed baseline estimate $\check{\xi}(N)$ are given by

$$\begin{aligned}\hat{N} &= (\bar{A}^{\mathrm{T}} \Sigma_\Psi^{-1} \bar{A})^{-1} \bar{A}^{\mathrm{T}} \Sigma_\Psi^{-1} P_H^{\perp} \tilde{\Psi} \\ \check{\xi}(N) &= (H^{\mathrm{T}} \Sigma_\Psi^{-1} H)^{-1} H^{\mathrm{T}} \Sigma_\Psi^{-1} (\tilde{\Psi} - AN). \end{aligned} \tag{9}$$

A sequential tree search shall now be performed for finding all relevant integer candidates. As the search tree is developed sequentially, the ambiguities are subdivided into a set of integer valued and a set of real-valued ambiguities. The real-valued set is attached to the baseline coordinates, i.e.

$$\tilde{N} = \begin{pmatrix} N^1 \\ \vdots \\ N^k \end{pmatrix} \in \mathbb{Z}^{k \times 1}, \quad \tilde{\xi} = \begin{pmatrix} \xi \\ N^{k+1} \\ \vdots \\ N^{K-1} \end{pmatrix} \in \mathbb{R}^{3+K-1-k}. \tag{10}$$

The elements of the two subsets also depend on the path in the search tree, which has been omitted to keep the notation simple. The error decomposition of Eq. (8) is now applied to the partially fixed solution, i.e.

$$\begin{aligned}\|\tilde{\Psi} - H\xi - AN\|^2_{\Sigma_\Psi^{-1}} =& \|\hat{\tilde{N}} - \tilde{N}\|^2_{\Sigma^{-1}_{\hat{\tilde{N}}}} + \|\check{\tilde{\xi}}(\tilde{N}) - \tilde{\xi}\|^2_{\Sigma^{-1}_{\check{\tilde{\xi}}(\tilde{N})}} \\ &+ \|P_{\bar{A}}^{\perp} P_H^{\perp} \tilde{\Psi}\|^2_{\Sigma_\Psi^{-1}}. \end{aligned} \tag{11}$$

The float ambiguities of the first term are in general correlated. These float ambiguities shall be related to the conditional ambiguities, which are uncorrelated and were derived by Teunissen in [2] as

$$\begin{aligned}&\hat{N}_{k|1,\ldots,k-1} \\ &= \hat{N}_k - \sum_{j=1}^{k-1} \frac{\sigma_{\hat{N}_k \hat{N}_{j|1,\ldots,j-1}}}{\sigma^2_{\hat{N}_{j|1,\ldots,j-1}}} \cdot (\hat{N}_{j|1,\ldots,j-1} - [\hat{N}_{j|1,\ldots,j-1}]), \end{aligned} \tag{12}$$

where the covariance $\sigma_{\hat{N}_k \hat{N}_{j|1,\ldots,j-1}}$ and variance $\sigma^2_{\hat{N}_{j|1,\ldots,j-1}}$ were derived by Teunissen in [2]. Eq. (12) enables us to rewrite the first component of Eq. (11) as

$$\|\hat{\tilde{N}} - \tilde{N}\|^2_{\Sigma^{-1}_{\hat{\tilde{N}}}} = \sum_{l=1}^{k} \frac{(\tilde{N}_l - \hat{\tilde{N}}_{l|1,\ldots,l-1})^2}{\sigma^2_{\hat{\tilde{N}}_{l|1,\ldots,l-1}}}. \tag{13}$$

Let $S = (1^{3\times 3},\ 0^{3\times K-1-k})$ select the baseline coordinates from the joint baseline/ ambiguity vector $\tilde{\xi}$. Combining Eq. (11), (13) and (7) then gives

$$\begin{aligned}\frac{(N_k - \hat{N}_{k|1,\ldots,k-1})^2}{\sigma^2_{\hat{N}_{k|1,\ldots,k-1}}} \leq\ & \chi^2 - \|P_{\bar{A}}^{\perp} P_H^{\perp} \tilde{\Psi}\|^2_{\Sigma_\Psi^{-1}} \\ & - \sum_{l=1}^{k-1} \frac{(N_l - \hat{N}_{l|1,\ldots,l-1})^2}{\sigma^2_{\hat{N}_{l|1,\ldots,l-1}}} \\ & - \min_{\tilde{\xi}} \left(\|\check{\tilde{\xi}}(\tilde{N}) - \tilde{\xi}\|^2_{\Sigma^{-1}_{\check{\tilde{\xi}}(\tilde{N})}} + \|S\tilde{\xi} - \bar{\xi}\|^2_{\Sigma^{-1}_{\bar{\xi}}} \right) \end{aligned} \tag{14}$$

The minimization of Eq. (14) provides the constrained partially fixed float solution given by

$$\check{\tilde{\xi}}_{\mathrm{opt}}(\tilde{N}) = \left(\Sigma^{-1}_{\tilde{\xi}} + S^{\mathrm{T}} \Sigma^{-1}_{\bar{\xi}} S \right)^{-1} \left(\Sigma^{-1}_{\tilde{\xi}} \check{\tilde{\xi}}(\tilde{N}) + S^{\mathrm{T}} \Sigma^{-1}_{\bar{\xi}} \bar{\xi} \right). \tag{15}$$

Solving the quadratic inequality of Eq. (14) for N_k yields a lower and an upper bound for the k-th ambiguity N_k:

$$\begin{aligned} l_{\hat{N}_k} &= \hat{N}_{k|1,\ldots,k-1} - \sigma_{\hat{N}_{k|1,\ldots,k-1}} \sqrt{A_k(\tilde{N})} \\ u_{\hat{N}_k} &= \hat{N}_{k|1,\ldots,k-1} + \sigma_{\hat{N}_{k|1,\ldots,k-1}} \sqrt{A_k(\tilde{N})}, \end{aligned} \tag{16}$$

with

$$\begin{aligned} A_k(\tilde{N}) = \chi^2 &- \|P_{\bar{A}}^{\perp} P_H^{\perp} \tilde{\Psi}\|^2_{\Sigma_\Psi^{-1}} - \sum_{l=1}^{k-1} \frac{(N_l - \hat{N}_{l|1,\ldots,l-1})^2}{\sigma^2_{\hat{N}_{l|1,\ldots,l-1}}} \\ &- \left(\|\check{\tilde{\xi}}(\tilde{N}) - \check{\tilde{\xi}}_{\mathrm{opt}}(\tilde{N})\|^2_{\Sigma^{-1}_{\check{\tilde{\xi}}(\tilde{N})}} + \|S\check{\tilde{\xi}}_{\mathrm{opt}}(\tilde{N}) - \bar{\xi}\|^2_{\Sigma^{-1}_{\bar{\xi}}} \right). \end{aligned} \tag{17}$$

The two terms in the second row of Eq. (17) describe the baseline measurement residuals and the baseline a priori residuals. The proposed estimate of Eq. (15) minimizes the sum of both weighted sum of squared errors (WSSE) and, thereby, finds the optimum trade-off between low baseline measurement residuals and low baseline a priori residuals. For the unconstrained integer search, the second term of the second row of Eq. (17) is not considered and $\check{\tilde{\xi}}_{\mathrm{opt}}(\tilde{N}) = \check{\tilde{\xi}}(\tilde{N})$ so that also the first term of the second row vanishes. The length of the search interval for N_k is obtained from Eq. (16) as

$$u_{\hat{N}_k} - l_{\hat{N}_k} = 2\sigma_{\hat{N}_{k|1,\ldots,k-1}} \sqrt{A_k(\tilde{N})}. \tag{18}$$

The substantial advantage of the soft-constrained integer search tree becomes obvious now: The subtraction of the last two terms from χ^2 in Eq. (17) substantially reduces the search space volume compared to the unconstrained integer search tree, and this dramatically improves the efficiency of the search.

The tree search is performed as follows: First, the search space volume is determined based on the unconstrained bootstrapping solution of Eq. (12) as

$$\chi^2 = \|\tilde{\Psi} - H\xi_{\mathrm{BS}} - AN_{\mathrm{BS}}\|^2_{\Sigma_\Psi^{-1}} + \|\xi_{\mathrm{BS}} - \bar{\xi}\|^2_{\Sigma^{-1}_{\bar{\xi}}}. \tag{19}$$

Subsequently, the constrained float solution is determined according to Eq. (15) and used to find A_1, $l_{\hat{N}_1}$ and $u_{\hat{N}_1}$ with Eq. (16) and (17). This defines the search interval for

the integer-valued N_1. For each of the integer candidates, a conditional partially fixed least-squares estimate $\check{\tilde{\xi}}_{\mathrm{opt}}(\tilde{N})$ of the baseline coordinates and remaining ambiguities is determined using Eq. (15), where $\tilde{N}$ denotes an integer candidate of the first ambiguity. Moreover, a conditional unconstrained float estimate $\hat{N}_{2|1}$ of the second ambiguity is computed based on Eq. (12). This enables us to determine $A_2(\tilde{N})$, $l_{\hat{N}_2}$ and $u_{\hat{N}_2}$, which provides search intervals for the second ambiguity conditioned on the candidates of the first ambiguity. A search tree evolves and is further developed until all candidates of the K-th ambiguity have been computed. Note that a branch in the search tree does not have to be further considered if $A_k(\tilde{N}) < 0$ as the search interval diminishes.

Once the search tree is completed, one selects the path whose respective ambiguities minimize the weighted sum of squared errors $\|\tilde{\Psi} - H\xi - AN\|^2_{\Sigma_\Psi^{-1}} + \|\xi - \bar{\xi}\|^2_{\Sigma_{\bar{\xi}}^{-1}}$. The obtained baseline/ ambiguities estimates represent then the solution of the MAP estimator.

B. Attitude determination and Coasting

The heading (yaw) angle is obtained from the MAP baseline estimate $\check{\tilde{\xi}}_{\mathrm{opt}}(\tilde{N})$ as:

$$\psi = \mathrm{atan}\left(\check{\tilde{\xi}}_{\mathrm{opt,E}}(\tilde{N}) / \check{\tilde{\xi}}_{\mathrm{opt,N}}(\tilde{N})\right), \tag{20}$$

and is counted clockwise with 0° in Northern direction. The elevation (pitch) angle is given by

$$\theta = \mathrm{atan}\left(\check{\tilde{\xi}}_{\mathrm{opt,U}}(\tilde{N}) / \sqrt{\check{\tilde{\xi}}^2_{\mathrm{opt,E}}(\tilde{N}) + \check{\tilde{\xi}}^2_{\mathrm{opt,N}}(\tilde{N})}\right). \tag{21}$$

Once the ambiguities are fixed, the constrained baseline solution can be easily coasted using Eq. (15) and $\check{\tilde{\xi}}(\tilde{N}) = \check{\xi}(\tilde{N})$ from Eq. (9).

C. Cycle Slip Detection and Correction

In the coasting phase, carrier phase measurements have to be carefully screened for cycle slips. As triple difference phase measurements do not enable a reliable cycle slip detection and correction during high receiver dynamics, the proposed MAP estimator shall also be used for cycle slip detection and correction. The MAP cycle slip correction follows as

$$\min_{\Delta N} \|\tilde{\Psi} - H\check{\xi}_{\mathrm{MAP}} - A(\check{N}_{\mathrm{MAP}} + \Delta N)\|^2_{\Sigma_\Psi^{-1}} + \|\check{\xi}_{\mathrm{MAP}} - \bar{\xi}\|^2_{\Sigma_{\bar{\xi}}^{-1}}, \tag{22}$$

where $\check{N}_{\mathrm{MAP}}$ and $\check{\xi}_{\mathrm{MAP}}$ are the MAP estimates of the initial ambiguity resolution and ΔN denotes the cycle slip correction for the current measurements $\tilde{\Psi}$. Relevant candidates for ΔN can be efficiently derived by predicting the triple difference carrier phases and comparing the predicted phases to the actual measured ones.

III. Measurement Analysis

The proposed MAP estimator of baseline coordinates and integer ambiguities was verified in a test drive, where two low-cost single frequency patch antennas were mounted on the roof of a car. Both antennas were aligned to the longitudinal axis of the car and had a negligible height difference. The baseline length was determined by a meter as 1.415 ± 0.005 m. Fig. 1 shows the track of the first test drive at Nymphenburg palace. The integer ambiguities were resolved in the beginning while the car was not moving. Thus, the orientation of the car was found without any movement. The subsequent track is subdivided into sections of 20 s.

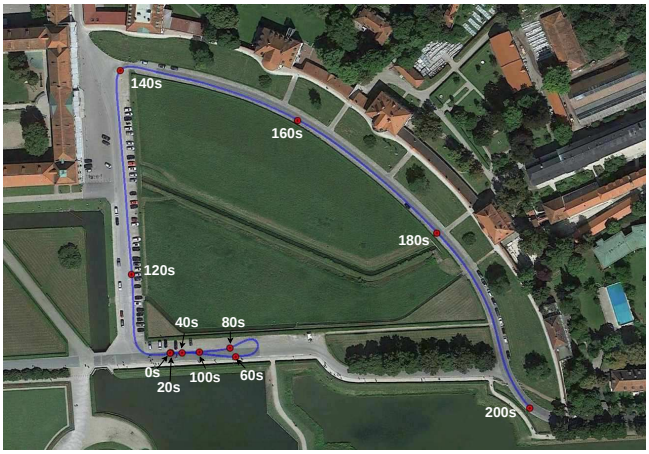

Fig. 1. Track of car drive at Nymphenburg palace. The integer ambiguities are resolved in the beginning while the car is not moving. The subsequent track is subdivided into sections of 20 s.

Fig. 2 shows the course of the heading during the test drive at Nymphenburg palace. The enlarged regions show that the noise of the heading estimate is in the order of only 0.1°. The abrupt heading changes at 70 s, 110 s and 140 s indicate u-turns or turns from one road into another road.

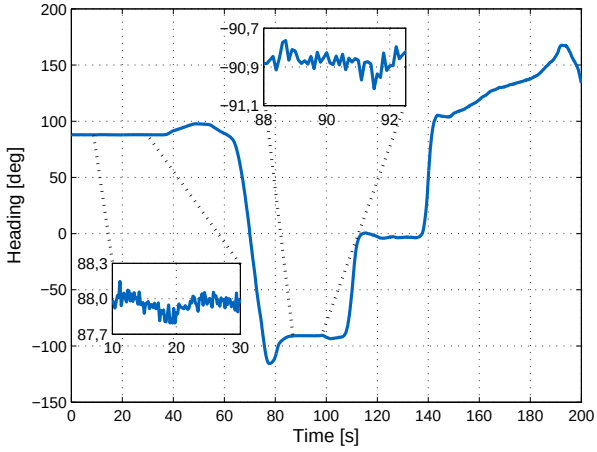

Fig. 2. Heading of track at Nymphenburg palace: The noise of the heading estimate is in the order of only 0.1°.

Fig. 3 shows the phase residuals of our MAP estimator for the track of Fig. 1. The phase residuals of the two satellites of highest elevation (PRN 29, 30) are only a few millimeters. The phase residuals of the other satellites are more affected by multipath but still remain unbiased and drift-free.

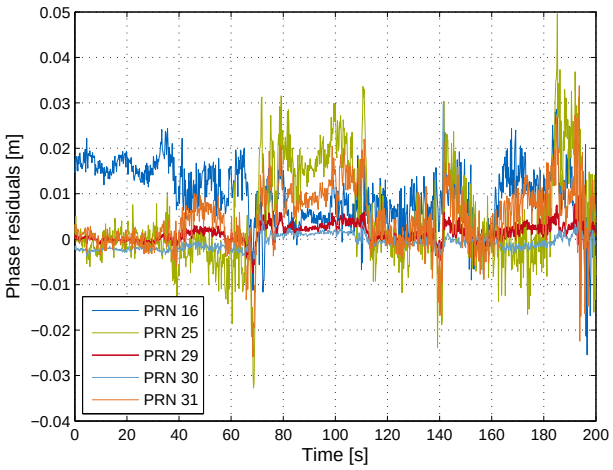

Fig. 3. Phase residuals of fixed baseline solution for track at Nymphenburg: The phase residuals of all satellites are far below one wavelength. For the two satellites of highest elevation, the residuals are only a few millimeters.

Fig. 4 shows the track of our second test drive in front of the ESA/ AZO building in Oberpfaffenhofen, Germany. The integer ambiguities were again resolved in the beginning while the car was standing. The track includes several turns and three sections with reversing at $97-104$ s, $140-160$ s and $180-185$ s. As the track was close to a high building, the code measurements were affected by substantial multipath.

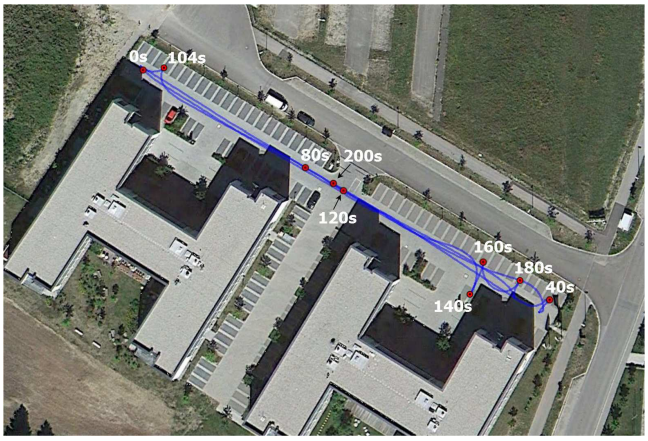

Fig. 4. Track of car drive in front of the ESA/ AZO building in Oberpfaffenhofen. The track includes three reverse drives at $97-104$ s, $140-160$ s and $180-185$ s

Fig. 5 shows the double difference phase residuals of the fixed MAP solution during the initial 160 s. The car was standing. The phase residuals of all 4 double differences are less than two centimeters over the complete period. This indicates a correct integer ambiguity resolution.

Fig. 6 shows the course of the heading as obtained by our MAP estimator. The estimated heading is varying only by a few degrees during the drive from one end to the other end of the road between 5 s and 35 s. The figure also shows three reversing sections in good agreement with Fig. 4.

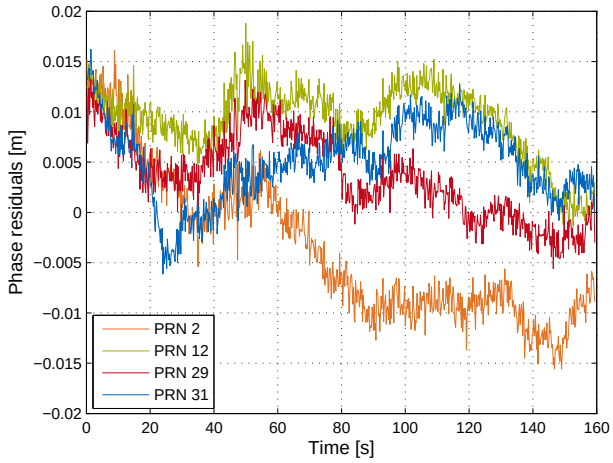

Fig. 5. Phase residuals during initial nteger ambiguity resolution.

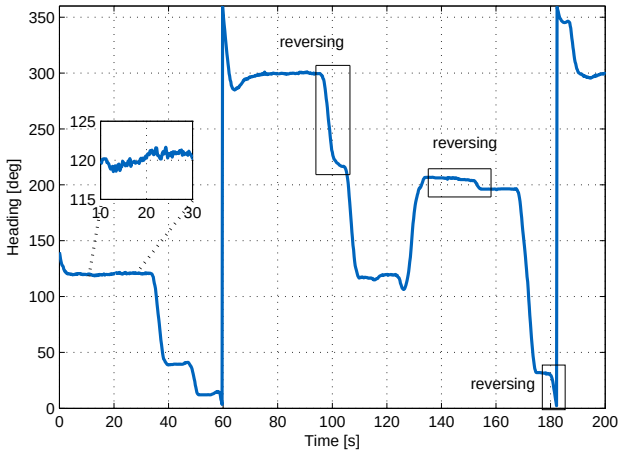

Fig. 6. Heading of car during car drive in front of the ESA/ AZO building.

IV. Conclusion

A maximum a posteriori probability estimator has been derived for relative carrier phase positioning, which fully integrates the baseline a priori information into the tree search.

References

[1] P. Henkel, G. Giorgi and C. Günther, *Precise Attitude Determination with Low Cost Satellite Navigation Receivers*, IEEE Transactions on Vehicular Technology, submitted, 2013.

[2] P. Teunissen, *The least-squares ambiguity decorrelation adjustment: a method for fast GPS ambiguity estimation*, J. of Geodesy, vol. 70, pp. 65-82, 1995.

[3] P. Teunissen, *Integer least-squares theory for the GNSS compass*, J. of Geodesy, vol. 84, pp. 433-447, 2010.

[4] P. Henkel and C. Günther, *Reliable Integer Ambiguity Resolution: Multi-Frequency Code Carrier Linear Combinations and Statistical A Priori Knowledge of Attitude*, Navigation, vol. 59, nr. 1, pp. 61-75, 2012.

[5] P. Henkel, *Bootstrapping with Multi-Frequency Mixed Code Carrier Linear Combinations and Partial Integer Decorrelation in the Presence of Biases*, Geodesy for Planet Earth, pp. 925-933, 2012.

[6] P. Henkel and C. Günther, *Partial integer decorrelation: optimum trade-off between variance reduction and bias amplification*, Journal of Geodesy, vol. 84, iss. 1, pp. 51-63, 2010.